

## Thermal dynamics of RNase A: unravelling interactions across varied temperatures in an in-silico exploration

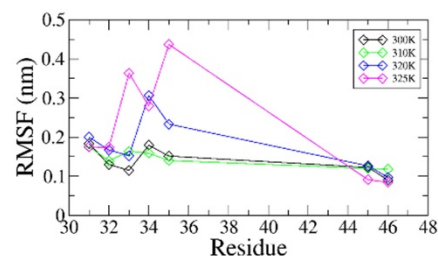
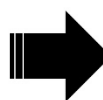
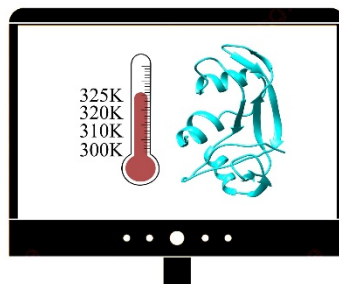
Ashal Ilyas, Subhomoi Borkotoky\*

Department of Biotechnology, Invertis University, Bareilly, India.

Submitted on: 01-Apr-2024, Accepted and Published on: 07-May-2024

Article

### ABSTRACT



RNase A stands as a pivotal molecule due to its multifaceted significance across diverse domains. Its unique enzymatic properties and well-characterized structure make it a model for studying protein folding, enzymatic catalysis, and the intricate relationship between structure and function in proteins. Beyond research, RNase A and its derivatives exhibit promising potential in cancer therapy, showcasing cytotoxic effects on tumour cells. Temperature-induced changes in proteins are pivotal as they profoundly influence their structure and function. Specifically, the study delves into the interactions of various ligands, such as A3P, ATP, trehalose, sucrose, glucosylglycerol, and ribonuclease inhibitor, with RNase A across a range of temperatures using different computational methods. Among the ligands tested, A3P, ATP, and trehalose exhibited robust interactions with RNase A across diverse thermal conditions, suggesting their potential role in modulating RNase A's behaviour. Moreover, the investigation underscores temperature-sensitive interactions between RNase A and ribonuclease inhibitor, revealing potential therapeutic implications for modulating cytotoxic effects while preserving thermal stability. This study investigates the influence of temperature on the flexibility, stability, and function of RNase A which is explored through computational simulations and molecular dynamics studies. The insights obtained from this study provide a deeper understanding of molecular relationships between diverse ligands and proteins across varying temperatures, suggesting promising avenues for future therapeutic applications.

**Keywords:** RNase A, Molecular Docking, MD Simulation, Osmolytes, Ribonuclease inhibitor, Temperature-induced Changes

### INTRODUCTION

Bovine pancreatic Ribonuclease A (RNase A) is an enzyme that catalyzes the cleavage of P-O5' bonds in RNA on the 3' side of pyrimidines. This enzymatic action results in the formation of cyclic 2',5'-phosphates. This property makes RNase A important in the context of RNA degradation and processing, as it specifically targets and cleaves RNA molecules at these positions, producing cyclic phosphate products.<sup>1</sup> Over time, RNase A has emerged as a molecular target for the development of small molecule inhibitors. These inhibitors are being designed to curb the biological activities of various RNase A homologs in a range of pathological conditions. These homologs encompass human Angiogenin (Ang), a potent inducer of neovascularization

associated with cancer, vascular diseases, and rheumatoid conditions, along with eosinophil-derived neurotoxin (EDN) and eosinophil cationic protein (ECP), which are neurotoxins implicated in hypereosinophilic syndromes and allergies. RNase A is an  $\alpha/\beta$  protein with more sheet than helical residues.<sup>2</sup> Variants of RNase A exhibit cytotoxicity even at low concentrations, unlike the native enzyme that shows cytotoxic effects only at exceptionally high levels. For instance, G88R RNase A, a monomeric variant replacing Gly88 with arginine, demonstrates toxicity to human leukemia cells. Further modification of G88R RNase A by replacing Lys7 with alanine (K7A/G88R RNase A) creates an even more potent toxin, highlighting the heightened cytotoxic potential of these variants.<sup>3-6</sup> The suggested mechanism underlying ribonuclease-induced cytotoxicity involves several stages: initial cell surface binding, internalization, translocation into the cytosol, evasion of cytosolic ribonuclease inhibitor protein (RI), and subsequent degradation of cellular RNA. Differences in the efficiency of these steps significantly impact the quantity of active ribonuclease within the cytosol, consequently influencing cell

\*Corresponding Author: Dr. Subhomoi Borkotoky  
Email: subhomoy.bk@gmail.com



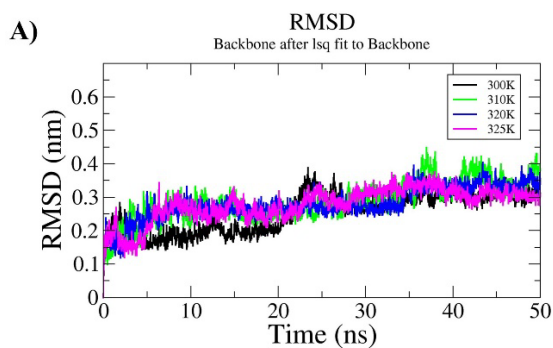
susceptibility to cytotoxicity.<sup>3</sup> Onconase® (ONC), an RNase A homolog, is being studied as a cancer chemotherapeutic treatment. The toxic impact of both ONC and variants of RNase A stems from their capacity to bypass the cytosolic ribonuclease inhibitor protein (RI) and break down cellular RNA.<sup>3</sup>

In silico exploration offers an exceptional avenue to delve into the complex molecular interactions governing enzyme's behaviour across a spectrum of temperatures, shedding light on the underlying mechanisms dictating its structural stability and functional dynamics.<sup>7-11</sup> A study conducted on SARS-CoV-2 reveals the effect of temperature on the spike protein of the virus through molecular dynamics simulation. The study includes the structural aspects of spike protein which can bind with human receptors.<sup>10</sup> Another study focused on the unfolding pattern of the trp-cage mini protein through molecular dynamics simulation.<sup>11</sup> Understanding the temperature-driven changes in RNase A's dynamics not only enhances our comprehension of protein thermodynamics but also holds implications for various industrial and biomedical applications. This work elucidates the critical interactions and adaptations of RNase A across diverse thermal environments through computational simulations. By employing molecular dynamics simulations and molecular docking methods, this study aims to unravel the temperature-induced alterations in the structural conformations, hydrogen bonding patterns, and overall dynamics of RNase A.

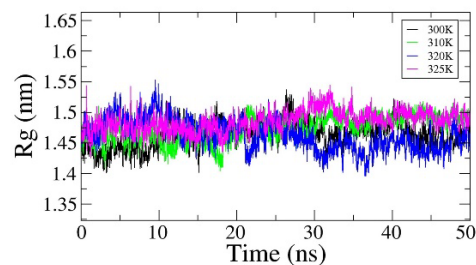
## RESULTS AND DISCUSSION

### Temperature dependent structural dynamics

The RNase A structure was simulated at four temperatures 300K (~27°C), 310K (~37°C), 320K (~47°C), and 325K (~52°C). From the RMSD (Root Mean Square Deviation) and Rg (Radius of gyration) profiles (Fig.1 A & B), no major deviation was observed in the structure at the selected temperature. To get further insights, RMSF profiles were analyzed. An earlier *in vitro* study<sup>12</sup> has revealed that the region spanning amino acids 31-35 and 45-46 is initially exposed during thermal unfolding, exhibiting increased flexibility. A previous *in vitro* study<sup>12</sup> has found the region between the amino acids 31-35 and 45-46 was first exposed during thermal unfolding and gained flexibility. A similar trend is observed in this study where increased flexibility was observed with average RMSF in the order 300K (0.12) < 310K (0.15) < 320K (0.16) < 325K (0.2) (Fig.1 C).



**B)** Radius of gyration (total and around axes)



**C)**

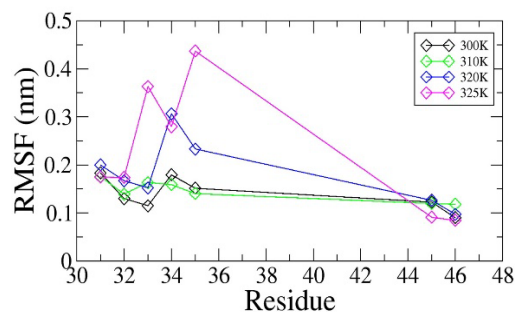


**Figure 1.** MD Simulation results: A) RMSD, B) Radius of gyration, C) RMSF of residues involved in thermal unfolding.

For further analysis, cartesian coordinate-based Principal Component Analysis (PCA) and Free Energy Landscape (FEL) analysis were performed to analyze the conformational dynamics and to extract minimum free-energy structures of RNase A at different temperatures. For this analysis, the final 30 ns trajectories were used. The FELs were generated after analyzing the first 20 projection eigenvectors at each temperature for their cosine content. From the contour maps at different temperatures, coordinates were collected from the largest minimum energy clusters, and the lowest energy representative structures corresponding to the coordinates were extracted. From the FEL analysis, it was observed that the RNase A is stable in the studied temperatures as evident from the single low energy basins and no major differences in the tertiary structures (Figure 2).

### MOLECULAR INTERACTIONS

The study employed molecular docking to assess how temperature-induced conformations interact with various binding partners. At 300K, A3P exhibited the highest binding energy (-6.3 kcal/mol), followed closely by ATP (-6.1 kcal/mol), trehalose (-5.3 kcal/mol), sucrose (-5.2 kcal/mol), and glucosylglycerol (-4.9 kcal/mol). Similarly, at the optimum 310K temperature, the trend remained consistent with A3P displaying the highest binding energy (-6.6 kcal/mol), followed by ATP (-6.1 kcal/mol), trehalose (-6.0 kcal/mol), sucrose (-5.5 kcal/mol), and glucosylglycerol (-5.5 kcal/mol). Upon elevating the temperature to 320K and 325K, A3P and ATP continued to demonstrate similar high binding energies (-6.2 kcal/mol and -6.3 kcal/mol,

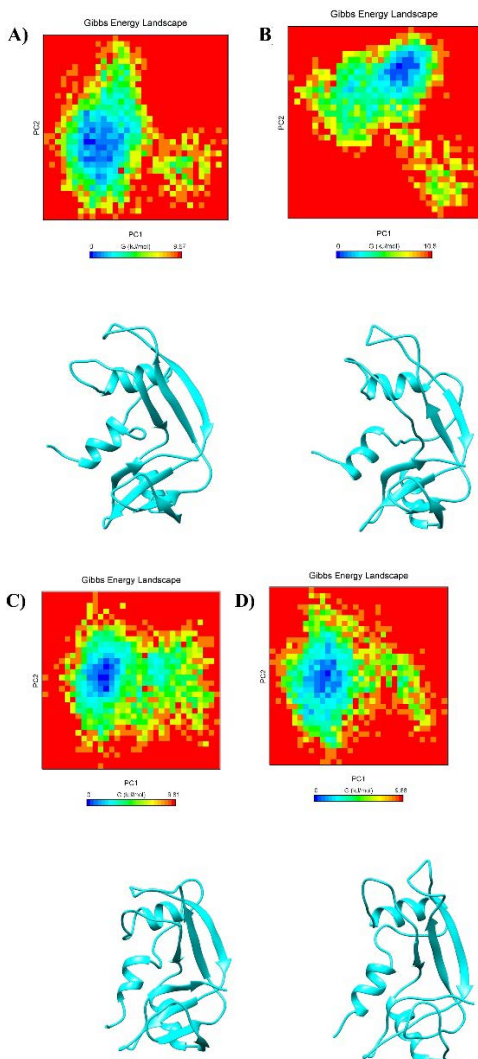


**Figure 2** FEL analyses of RNase A depicting low energy basin along with the representative structure retrieved at each temperature: A) 300K, B) 310K, C) 320K and D) 325K.

respectively), whereas the energies for trehalose, sucrose, and glucosylglycerol showed fluctuations (Table 1). In essence, the results consistently highlight that RNase A exhibits the maximum binding affinity with A3P and ATP across various temperature ranges, indicating their strong interaction and potential significance in molecular associations at different thermal conditions.

Among osmolytes, trehalose interacted with RNase A at all temperatures more strongly than other osmolytes. This observation is consistent with the previous study which shows the presence of trehalose enhances the thermal stability of RNase A<sup>13</sup>. While both sucrose and glucosylglycerol exhibit varying binding energies across the range of temperatures, a notable observation emerges at 310K and 325K. At 310K, both sucrose and glucosylglycerol showcase equally strong binding energies of -5.5 kcal/mol, indicating robust interactions with RNase A at this temperature. However, at 325K, while sucrose maintains a

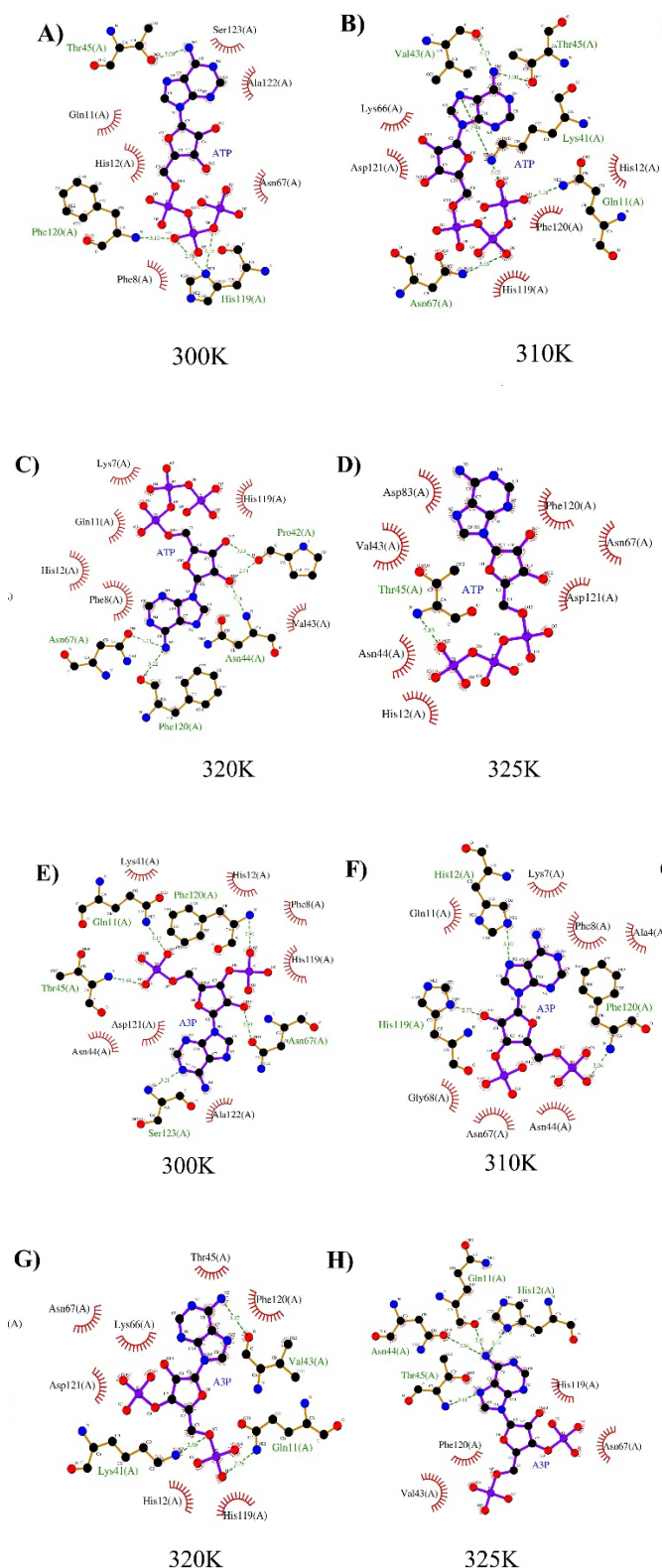


**Figure 3** The 2D interaction pattern of ATP (upper panel) and A3P (lower panel) docked to different temperature induced conformations of RNase A.

high binding energy of -5.5 kcal/mol, glucosylglycerol's interaction slightly decreases to -5.1 kcal/mol. This indicates that at 325K, glucosylglycerol's affinity for RNase A weakens compared to its interaction at 310K and to Sucrose's interaction at 325K. Therefore, while both osmolytes exhibit the highest interactions at 310K, Glucosylglycerol's interaction with RNase A shows a relatively decreased affinity at 325K compared to its interaction at 310K and to Sucrose's interaction at 325K. (Table 1). All the ligands interacted with the critical residues of RNase A (Figure 3-5).

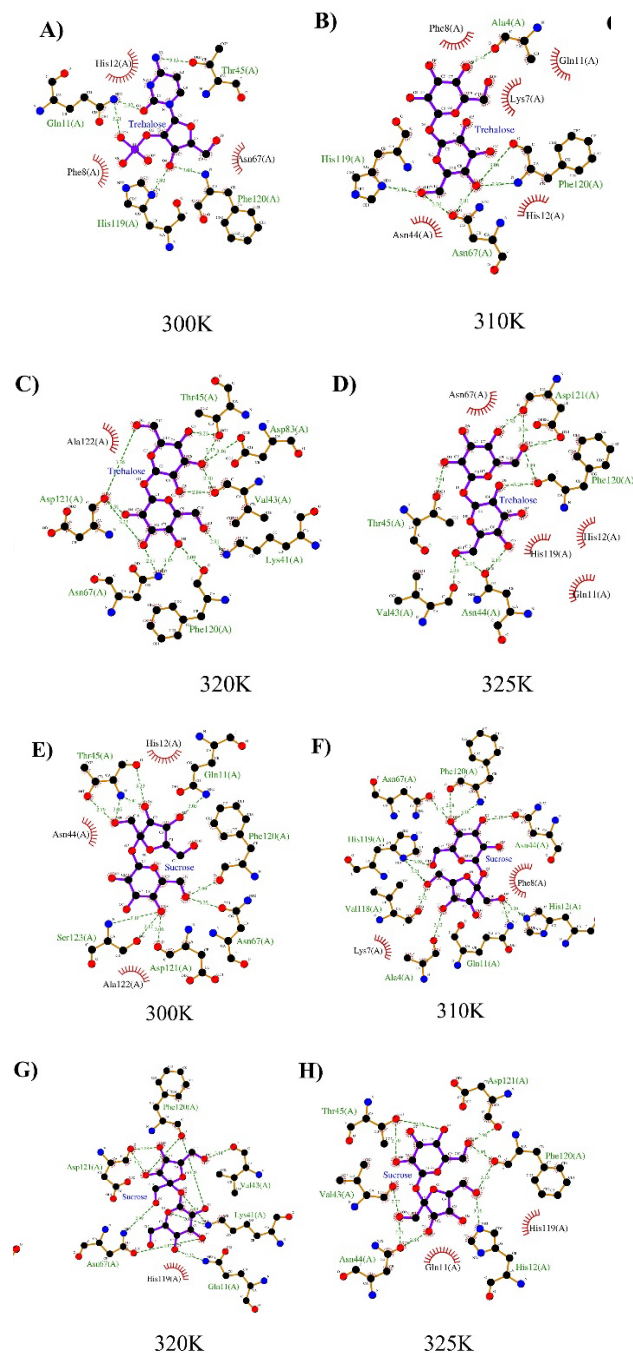


**Figure 4** The 2D interaction pattern of Trehalose (upper panel) and Sucrose (lower panel) docked to different temperature induced conformations of RNase A.

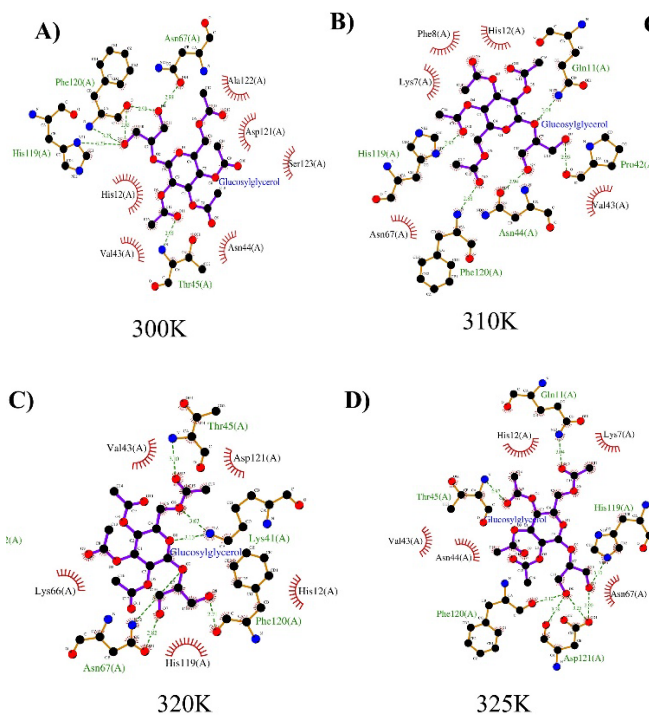
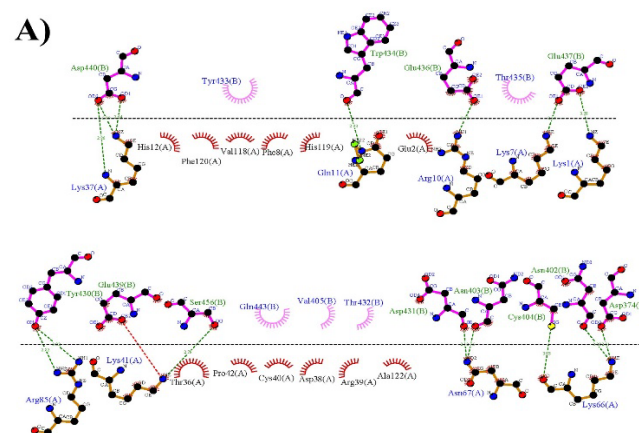


**Figure 5** The 2D interaction pattern of glucosylglycerol docked to different temperature induced conformations of RNase A.

Following the docking of RNase A structures at various temperatures with RI via the HADDOCK server, Table 2 highlights the most favorable interaction models. These models were selected based on their HADDOCK score and binding energy. At 310K, the RI exhibited the most robust interaction with RNase A, displaying the highest HADDOCK score ( $-135.7 \pm 7.7$ ) and binding energy ( $-12.8$  kcal/mol) among the temperatures tested. The subsequent notable interaction was at 320K, recording a HADDOCK score of  $-121.2 \pm 14.3$  and a binding energy of  $-12.1$  kcal/mol. Comparatively lower scores and energies were observed at 300K ( $-113.1 \pm 12.9$  &  $-10.9$  kcal/mol) and 325K ( $-98.2 \pm 3.4$  &  $-10.1$  kcal/mol), indicating reduced affinity in contrast to the optimal 310K temperature.





from the crystal structure of RNase A-5'-ATP complex (PDB ID: 2W5G).<sup>24</sup> Two osmolytes glucosylglycerol (PubChem ID: 131700592) and sucrose (PubChem ID: 5988) were also used as ligands. These two osmolytes were previously proposed to be strong binders to RNase A.<sup>25</sup> Another osmolyte, trehalose in which the presence RNase A became more resistant to denaturation or maintained its structural stability at higher temperatures across various pH ranges.<sup>13</sup>

In addition to these various inhibitors were also studied. One inhibitor, adenylic inhibitor 3',5'-ADP (A3P), which was obtained from the crystal structure of RNase A in complex with 3',5'-ADP (PDB ID: 1OOF).<sup>2</sup> The Ribonuclease inhibitor (RI), a cytosolic protein, structure was obtained from the RNase A-RI complex (PDB ID: 1DFJ).<sup>5</sup> The protein-protein docking was performed using HADDOCK (High Ambiguity Driven protein-protein DOCKing) server.<sup>26</sup> HADDOCK is a widely used docking program, that employs a data-driven approach, and accommodates diverse experimental data for protein-protein docking. For the docking process, the residues for RNase A (Lys 7, Gln 11, Asp 38, Lys 66, Asn 67, Asn 71, Ser 89, Glu 111) and RI (Glu 202, Cys 404, Val 405, Tyr 433, Arg 453, Ser 456) were selected as active residues based on the RNase A-RI complex crystal structure. The passive residues were automatically defined around the active residues. The binding energy was calculated using the PRODIGY (PROtein binDing enerGY prediction) server.<sup>27-29</sup>

## CONCLUSION

Proteins rely on structural changes for their vital biological functions<sup>14-16</sup>. Enzymes, pivotal for binding substrates, triggering reactions, and releasing products, often undergo structural adaptations. However, increased flexibility typically trades off with thermodynamic stability. Temperature significantly governs a protein's flexibility, stability, and overall shape, dictating its function.<sup>17,18</sup> Computational simulations and molecular dynamics studies have played a pivotal role in unravelling these complex protein behaviours.<sup>9</sup> For instance, a comparative exploration of molecular dynamics simulations involving five RNase H homologs, each exhibiting distinct thermostabilities and activities at room temperature. These simulations unveil consistent dynamic processes in the RNase H handle region, shedding light on how these motions impact substrate binding and identifying critical residues that regulate these mechanisms.<sup>17</sup>

In this investigation of RNase A interactions with different ligands across varying temperatures, A3P and ATP consistently exhibited the highest binding energies, suggesting robust and persistent interactions with RNase A across diverse thermal conditions. Trehalose consistently displayed stronger affinities with RNase A compared to other osmolytes at all temperatures, aligning with prior studies indicating its role in enhancing RNase A's thermal stability. Notably, while both sucrose and glucosylglycerol showcased similar strong interactions with RNase A at 310K, glucosylglycerol's affinity weakened at 325K compared to its interaction at 310K and sucrose's interaction at 325K. These results shed light on distinct ligand-protein interactions, emphasizing the potential significance of A3P, ATP,

and trehalose in modulating RNase A's behaviour across varying thermal environments.

The diverse binding energies observed during the docking of Ribonuclease Inhibitor (RI) with RNase A across temperatures (300K, 310K, 320K, and 325K) underscore the temperature-sensitive nature of their interaction. The affinity of a ribonuclease for RI plays an integral role in defining the potency of a cytotoxic effect of ribonuclease. An earlier study<sup>5</sup> highlights the significance of preserving the native conformation of ribonucleases for eliciting cytotoxic responses at physiological temperature and RNase A is not cytotoxic when binds to RI with high affinity. Specifically, engineered alterations in RNase A were aimed at diminishing its interaction with RI while safeguarding its thermal stability. In this study, docking RI with RNase A structures at varying temperatures revealed the highest binding energy at 310K (-12.8 kcal/mol), closely followed by 320K (-12.1 kcal/mol). The minimal difference in binding energy between 310K and 320K suggests a robust interaction even at both temperatures. Furthermore, our MD simulations demonstrated that RNase A remained stable across all tested temperatures. Hence, the results suggest that the cytotoxic effect of RNase A can be inhibited by RI at both 310K and 320K without compromising thermal stability.

In conclusion, this study could be pivotal in unraveling the intricate molecular relationships between diverse ligands and RNase A across fluctuating temperatures, offering promising avenues for future therapeutic applications.

## ACKNOWLEDGMENTS

The authors acknowledge Department of Biotechnology, Invertis University for providing necessary facilities.

## REFERENCES

1. M. Moussaoui, C.M. Cuchillo, M.V. Nogue. A phosphate-binding subsite in bovine pancreatic ribonuclease A can be converted into a very efficient catalytic site. *Protein Sci* **2007**, 16(1), 99-109.
2. D.D. Leonidas, G.B. Chavali, N.G. Oikonomakos et. al. High-resolution crystal structures of ribonuclease A complexed with adenylic and uridylic nucleotide inhibitors. Implications for structure-based design of ribonucleolytic inhibitors. *Protein Sci* **2003**, 12(11), 2559-74.
3. M.C. Haigis, E.L. Kurten, R.T. Raines. Ribonuclease inhibitor as an intracellular sentry. *Nucleic Acids Res* **2003**, 31(3), 1024-32.
4. L. Ledoux. Action of ribonuclease on certain ascites tumours. *Nature* **1955**, 175(4449), 258-9.
5. P.A. Leland, L.W. Schultz, B.M. Kim, R.T. Raines. Ribonuclease A variants with potent cytotoxic activity. *Proc Natl Acad Sci U S A* **1998**, 95(18), 10407-12.
6. M.C. Haigis, E.L. Kurten, R.L. Abel, R.T. Raines. KFERQ sequence in ribonuclease A-mediated cytotoxicity. *J Biol Chem* **2002**, 277(13), 11576-81.
7. S.K. Bharatiy, M. Hazra, M. Paul et. al. In Silico Designing of an Industrially Sustainable Carbonic Anhydrase Using Molecular Dynamics Simulation. *ACS Omega* **2016**, 1(6), 1081-103.
8. N. Rai, A. Ramaswamy. Temperature dependent dynamics of DegP-trimer: A molecular dynamics study. *Comput Struct Biotechnol J* **2015**, 13329-38.
9. M. Dong. A Minireview on Temperature Dependent Protein Conformational Sampling. *Protein J* **2021**, 40(4), 545-53.
10. S.L. Rath, K. Kumar. Investigation of the Effect of Temperature on the Structure of SARS-CoV-2 Spike Protein by Molecular Dynamics Simulations. *Front Mol Biosci* **2020**, 7583523.

11. A.S. Seshasayee. High-temperature unfolding of a trp-cage mini-protein: a molecular dynamics simulation study. *Theor Biol Med Model* **2005**, 27.
12. U. Arnold, K.P. Rucknagel, A. Schierhorn, R. Ulbrich-Hofmann. Thermal unfolding and proteolytic susceptibility of ribonuclease A. *Eur J Biochem* **1996**, 237(3), 862-9.
13. T.Q. Faria, S. Knapp, R. Ladenstein et. al. Protein stabilisation by compatible solutes: effect of mannosylglycerate on unfolding thermodynamics and activity of ribonuclease A. *Chembiochem* **2003**, 4(8), 734-41.
14. D. Tikhonov, L. Kulikova, V. Rudnev et. al. Changes in Protein Structural Motifs upon Post-Translational Modification in Kidney Cancer. *Diagnostics (Basel)* **2021**, 11(10).
15. S. Borkotoky, D. Dey. Structural investigations of the palmitoylated F13 envelope protein of Mpox virus. *J Med Virol* **2023**, 95(5), e28798.
16. K.S. Nikolsky, L.I. Kulikova, D.V. Petrovskiy et. al. Analysis of Structural Changes in the Protein near the Phosphorylation Site. *Biomolecules* **2023**, 13(11).
17. K.A. Stafford, P. Robustelli, A.G. Palmer, 3rd. Thermal adaptation of conformational dynamics in ribonuclease H. *PLoS Comput Biol* **2013**, 9(10), e1003218.
18. M. Vihinen. Relationship of protein flexibility to thermostability. *Protein Eng* **1987**, 1(6), 477-80.
19. A. Talukder, M.M. Rahman, M.H.U. Masum. Biocomputational characterisation of MBO\_200107 protein of Mycobacterium tuberculosis variant caprae: a molecular docking and simulation study. *Journal of Biomolecular Structure and Dynamics* **2023**, 41(15), 7204-23.
20. N. Schmid, A.P. Eichenberger, A. Choutko et. al. Definition and testing of the GROMOS force-field versions 54A7 and 54B7. *Eur Biophys J* **2011**, 40(7), 843-56.
21. G.G. Maisuradze, D.M. Leitner. Free energy landscape of a biomolecule in dihedral principal component space: sampling convergence and correspondence between structures and minima. *Proteins* **2007**, 67(3), 569-78.
22. S. Borkotoky, C. Kumar Meena, G.M. Bhalerao, A. Murali. An in-silico glimpse into the pH dependent structural changes of T7 RNA polymerase: a protein with simplicity. *Sci Rep* **2017**, 7(1), 6290.
23. M.S. Valdes-Tresanco, M.E. Valdes-Tresanco, P.A. Valiente, E. Moreno. AMDock: a versatile graphical tool for assisting molecular docking with Autodock Vina and Autodock4. *Biol Direct* **2020**, 15(1), 12.
24. D.E. Holloway, G.B. Chavali, D.D. Leonidas et. al. Influence of naturally-occurring 5'-pyrophosphate-linked substituents on the binding of adenylic inhibitors to ribonuclease a: an X-ray crystallographic study. *Biopolymers* **2009**, 91(12), 995-1008.
25. A. Ilyas, N.K. Poddar, S. Borkotoky. Insights into the dynamic interactions of RNase a and osmolytes through computational approaches. *Journal of Biomolecular Structure and Dynamics* 1-9.
26. S.J. de Vries, M. van Dijk, A.M. Bonvin. The HADDOCK web server for data-driven biomolecular docking. *Nat Protoc* **2010**, 5(5), 883-97.
27. L.C. Xue, J.P. Rodrigues, P.L. Kastiris et. al. PRODIGY: a web server for predicting the binding affinity of protein-protein complexes. *Bioinformatics* **2016**, 32(23), 3676-78.
28. S. Sharma, Y. Monga, A. Gupta, S. Singh. In silico screening and molecular docking study of quinoline based compounds with Human kallikrein 7 in complex with 1,4-diazepane-7-one 1-acetamide derivative receptor target for potential antibacterials. *J. Mol. Chem.* **2023**, 3 (1), 585.
29. V.K. Maurya, S. Kumar, M. Singh, V. Saxena. Molecular docking and dynamic studies of novel phytoconstituents in an investigation of the potential inhibition of protein kinase C- beta II in diabetic neuropathy. *J. Mol. Chem.* **2023**, 3 (2), 589.